

A MESH ADAPTATION ALGORITHM TO REDUCE MESH BIAS IN 2D AND 3D CRACK PROPAGATION ANALYSIS USING COHESIVE ZONE MODELS

KOUSSAY DAADOUC^{*}, VLADISLAV GUDŽULIĆ^{*} AND GÜNTHER MESCHKE^{*}

^{*}Ruhr University Bochum, Institute for Structural Mechanics
Universitätsstraße 150, 44801 Bochum, Germany
e-mail: koussay.daadouch@rub.de, www.sd.rub.de

Key words: Cohesive Zone Method, Interface Elements, Mesh Reorientation, Mesh Bias.

Abstract. This paper presents a novel mesh reorientation algorithm that enhances the reliability of crack path prediction in cohesive zone cracking models by reducing the inherent mesh bias. The proposed method realigns interface elements to maximize their local tensile traction, facilitating cracking in energetically more favorable direction. Extensive testing shows that the algorithm consistently improves results in 2D and 3D applications, enabling more reliable predictions, including cracks originating within the domain, without requiring crack tracking or pre-specifying crack initiation points.

1 INTRODUCTION

A prevalent technique in finite element modeling for simulating fractures in brittle and quasi-brittle materials involves the use of cohesive zone models with zero-thickness interface elements [1]. This method enables a set of advantages, namely the discrete representation of cracks without the need of regularization techniques and the ability to handle multiple cracks, crack branching and coalescing. Moreover, interface elements allow for simple modeling of crack closure. Not to mention, that different traction-separation relations can be integrated within the interface elements and can be reliably used in simulations from the meso- to the structural-scale [2, 3].

One significant limitation of using interface elements is the high computational load, primarily due to the duplication of nodes when interface elements are inserted in the finite element mesh between every two adjacent continuum elements. To mitigate the computational burden, a well-established strategy is the adaptive insertion of interface elements during analysis, where they are inserted on-the-fly only

where and when they are needed, effectively reducing the number of nodes duplication and, consequently, computational demand [4].

Since cracks have to follow mesh-dependent paths along the boundaries of continuum elements, predicting crack propagation with interface elements poses a second challenge, which is mesh-biased results. Some strategies have been proposed to diminish this bias in the crack paths of two-dimensional finite element models, see e.g., [5]. These methods involve repositioning elements to align their edges in directions determined by stress or energy criteria, e.g, configurational forces. Nonetheless, such methods can only handle cases where a crack originates from a notch or a pre-defined node and by keeping track of the advancing crack front. For 3D problems, no reliable solution is available to the best knowledge of the authors.

This contribution introduces a computational approach for predicting crack initiation and propagation in both two- and three-dimensional finite element models. This is achieved through the adaptive insertion of interface elements, which are augmented with a cohesive law and

a crack path prediction mechanism based on local traction of interface elements. The mesh is then adaptively adjusted by slightly moving the nodes, which reorients the interface elements such that they align with the computed crack path. The efficacy of this method is validated through classic benchmarks, including the L-shaped panel and the single-edge notched tension and shear tests. In addition, we demonstrate the method's capability to predict cracks originating within the domain, not from a notch or the domain's boundary, by modeling the cylinder splitting test.

This paper briefly explores the finite element formulation of the used interface elements and their traction separation relation in Section 2. In Section 3, we present the algorithms for adaptive insertion of interface elements and adaptive mesh reorientation. The simulation results of several benchmarks are discussed in Section 4.

2 MODEL FORMULATION

We model the solid body as homogeneous linear elastic and discretize it with standard small-displacements Lagrangian elements: 3-node triangles in 2D and 4-node tetrahedrons in 3D. To model fracture of the body, we insert zero-thickness interface elements equipped with an intrinsic traction-separation law. We utilize 4-node line interface elements in 2D (Figure 1-a) and 6-node triangular interface elements in 3D (Figure 1-b). Each interface element bridges two adjacent continuum elements and represents a crack when it is damaged [1,3].

The cohesive law governing these interface elements is linear intrinsic, characterized by a high penalty stiffness K_c^{pen} in the linear elastic region (Figure 1-c). This stiffness ensures that intact interface elements have negligible influence on the overall system response.

The interface element remains intact until its effective traction, \bar{t}_c , reaches the material's tensile strength f_{tu} . At this point, damage initiates, and the interface enters the softening phase and begins to open, simulating the formation of a crack. The effective traction \bar{t}_c and the effective opening $\bar{\delta}_c$ of the interface are calculated based

on the local projections of the traction vector and opening onto the interface's local axes, expressed as:

$$\begin{aligned}\bar{t}_c(\mathbf{t}) &= \sqrt{\langle t_{cx'} \rangle_+^2 + \frac{1}{\beta^2}(t_{cy'}^2 + t_{cz'}^2)}, \\ \bar{\delta}_c &= \sqrt{\langle [u_{x'}] \rangle_+^2 + \frac{\beta^2}{\kappa^2}([\![u_{y'}]\!]^2 + [\![u_{z'}]\!]^2)},\end{aligned}\quad (1)$$

where $\langle \bullet \rangle_+$ denotes Macauley brackets, $t_{cx'}$, $t_{cy'}$, and $t_{cz'}$ are the local components of the traction vector \mathbf{t} , and $[\![u_{x'}]\!]$, $[\![u_{y'}]\!]$, and $[\![u_{z'}]\!]$ are the local components of the interface's opening. The parameter β is the ratio of shear to tensile strength ($\beta = \frac{f_{su}}{f_{tu}}$), and κ is the ratio of mode II to mode I fracture energies ($\kappa = \frac{G_{F,II}}{G_{F,I}}$).

The damage variable d characterizes the degradation of the interface element, $d = \min(1 - \frac{q_c}{K_c \delta_{\max}}, 1)$, ranging from 0 to 1. When the interface is intact, $d = 0$. As the effective traction \bar{t}_c reaches the tensile strength f_{tu} , damage begins, and d increases. During this phase, the element experiences softening, with its stiffness reducing according to the relation $K_c = (1 - d)K_c^{\text{pen}}$. When the effective opening $\bar{\delta}_c$ reaches the maximum opening δ_{\max} , complete decohesion occurs, at which point $d = 1$.

The maximum opening δ_{\max} is calculated as:

$$\delta_{\max} = \frac{2G_{F,I}}{f_{tu}} + \frac{f_{tu}}{K_c^{\text{pen}}}. \quad (2)$$

The failure surface in the traction space, shown in Figure 1-d, is defined as:

$$\begin{aligned}\hat{F}_c(\mathbf{t}, q_c) &= \bar{t}_c - q_c \leq 0, \\ q_c(\bar{\delta}_c) &= f_{tu} \frac{\delta_{\max} - \delta_0}{\bar{\delta}_c - \delta_0},\end{aligned}\quad (3)$$

where $\delta_0 = f_{tu}/K_c^{\text{pen}}$.

In essence, the behavior of intrinsic interface elements follows a well-defined progression: initially, they act as intact, highly stiff elements that do not alter the system's response. As loading increases, some of these elements may reach their tensile strength, leading to damage initiation, softening and opening, simulating crack development.

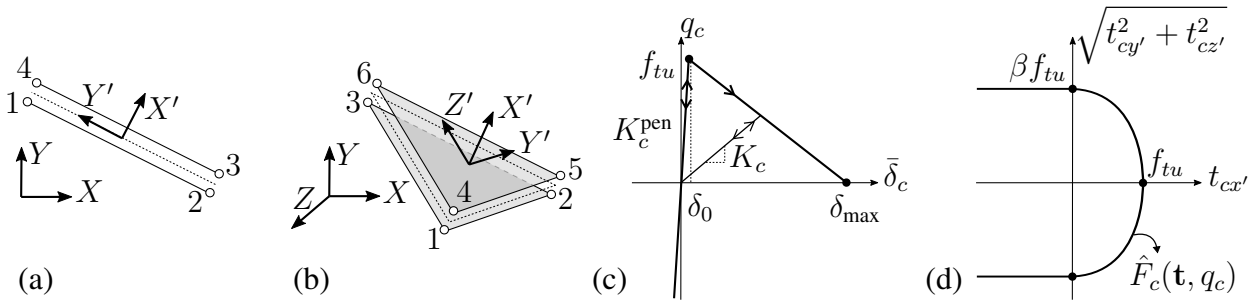


Figure 1: (a) 4-node line interface element in 2D with its local axes. (b) 6-node triangular interface element in 3D with its local axes. (c) Linear intrinsic traction-separation law. (d) Failure surface in the traction space.

3 MESH ADAPTATION ALGORITHMS

To improve the usability and reliability of the cohesive cracking models with interface elements, we use two algorithms: adaptive insertion of interface elements and adaptive mesh re-orientation. These algorithms are executed after finding the solution of every load step, and are independent, i.e., we can run one algorithm without the other if needed.

3.1 Adaptive Insertion of Interface Elements

To reduce computational cost associated with duplicated nodes of a priori inserting interface elements in the domain, we adaptively insert interfaces only where and when they are needed. This approach significantly reduces node duplication and is based on the efficient method proposed in [4], which leverages a compact, adjacency-based topological data structure [6]. This data structure efficiently stores necessary information while allowing quick retrieval of adjacency data, crucial for mesh updates.

An interface element is inserted in the facet between two adjacent continuum elements. The insertion criterion determines when to insert the element based on the facet's traction $\mathbf{t} = \boldsymbol{\sigma} \cdot \mathbf{n}$, where $\boldsymbol{\sigma}$ is the stress tensor projected on that facet and \mathbf{n} is the facet's normal vector. When the facet's effective traction \bar{t} (see Equation 1), exceeds the critical value $k f_{tu}$, the facet is flagged and an interface element is inserted. The insertion factor, k , chosen between 0.6 and 0.8, ensures reliable insertion of interface elements by accounting for potential stress field in-

accuracies. Setting $k = 0$ means pre-inserting interface elements in the entire domain. Worth noting is that, we insert intact interface elements that do not affect the overall behavior of the structure. The actual cracking, i.e., opening of the interface elements, might occur later when their failure criterion is met (see Equation 3).

Inserting an interface element requires first retrieving adjacency information of the flagged facet to determine which nodes need to be duplicated. Upon duplicating the nodes and inserting the interface element, the connectivity of the mesh has to be updated to reflect the new changes (for details refer to [4, 7]).

3.2 Adaptive Mesh Reorientation

The goal of this work is to develop a method that improves the reliability of interface elements in predicting crack paths while reducing mesh dependency. This method should be applicable in both 2D and 3D scenarios and capable of handling multiple cracks, including branching and coalescence, without the need for crack tracking. Additionally, it should predict cracks originating within the solid domain, not just from notches (singularities) or boundaries. Rather than aiming for perfect crack trajectories, the focus is on enhancing results obtained from poorly shaped meshes and minimizing mesh bias.

The algorithm works by optimizing the orientation of intact interface elements. Every intact interface experiences traction as it bridges two continuum elements. The traction is a vector that has normal and tangential components

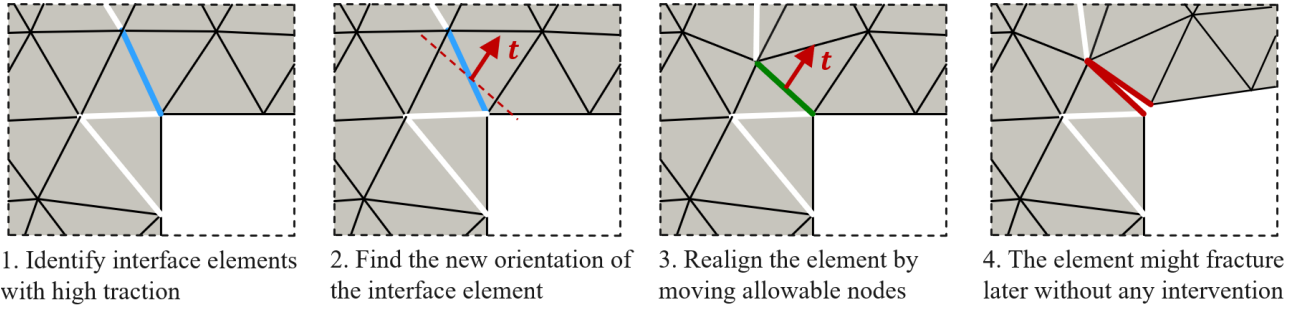


Figure 2: Adaptive mesh reorientation algorithm. White, blue, green and red indicate intact, flagged, reoriented and opened interface elements, respectively.

when projected onto the local axis of the interface element. Slightly changing the orientation of the interface element marginally affects the traction vector, however, it can significantly alter its local components projected onto the interface. Exploiting this, we can carefully orient an interface element such that we maximize its normal tensile traction. Since the traction-separation law we are using favors cracking under pure tensile traction (mode I), orienting the element to maximize its tensile traction allows for cracking with less energy. This reduces the mesh-bias as we allow the solid body to develop energetically more favorable cracks compared to the same scenarios without reorientation. In essence this method primarily promotes mode I cracking but does not eliminate mode II or mixed-mode cracking; it simply allows elements on the verge of mode I cracking to crack in a more energetically favorable orientation. The algorithm is summarized as follows and is depicted in Figure 2.

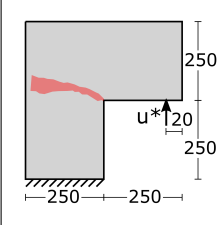
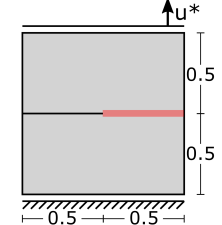
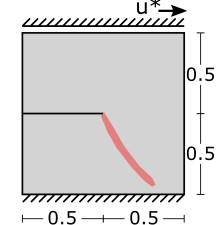
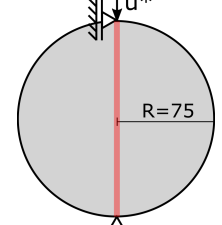
1. After finding the solution of the current load-step, compute the traction of all intact interface elements. The intact interfaces that have a tensile traction higher than the tensile strength reduced by a factor (ranging from 0.5 to 0.8), are flagged for realignment.
2. For every flagged interface we compute the new orientation of the element such that the tensile traction is maximized, i.e, the element is perpendicular to its traction. The new orientation is defined by a line in 2D and a surface in 3D.

3. To realign an interface element, we first check the movability of its nodes. Nodes are not allowed to move if they cause ill-shaped elements in the vicinity, affect opened (damaged) interface elements or if they change the boundary or boundary conditions of the model. For example, in Figure 2-3, the corner node is not allowed to move, while the inner node of the flagged interface is. Then the movable nodes are moved to align the interface in the pre-calculated orientation. A simple mesh smoothing is performed to the mesh in the vicinity of the moved nodes to insure a good quality mesh.
4. We continue the analysis with further load-steps. When an interface experience high traction, triggering its damage criterion, it starts to open without any further intervention from the mesh reorientation algorithm.

4 RESULTS

This section presents the results obtained using the adaptive mesh reorientation scheme across a series of standard benchmarks. Table 1 lists the simulated benchmarks, detailing their geometry, boundary conditions, expected crack paths (drawn in red), and material properties. The chosen benchmarks and their expected crack paths are well-documented in the literature, e.g., [8, 9], and the material properties are specifically adapted here for use with the cohesive crack model. The presented cylinder splitting test (Table 1) is improvised to demonstrate the capability of the method to predict cracks originating from within the domain.

Table 1: Simulated benchmarks

Benchmark	L-shaped panel	Single-edge notched tension		Single-edge notched shear		Cylinder splitting
Geometry and boundary conditions <i>Dimensions in mm</i> <i>Expected crack path shown in red</i>						
Dimension	2D	2D	3D	2D	3D	2D
Thickness	100 mm	1 mm	0.2mm	1 mm	0.2mm	1 mm
Elastic modulus	20000 N/mm ²	210000 N/mm ²		210000 N/mm ²		30000 N/mm ²
Poisson's ratio	0.18	0.299999		0.299999		0.2
Tensile strength	2.7 N/mm ²	500 N/mm ²		500 N/mm ²		2 N/mm ²
Fracture energy	0.095 N/mm	0.1 N/mm		0.1 N/mm		0.06 N/mm
	$\beta = 10, \kappa = 10$	$\beta = 1, \kappa = 1$		$\beta = 1, \kappa = 1$		$\beta = 50, \kappa = 10$

The objective of this testing campaign is not to compare the cohesive crack model to other models. Instead, the focus is on demonstrating how the proposed adaptive mesh reorientation scheme enhances the crack prediction capabilities of the cohesive zone crack model. This improvement leads to more accurate crack paths, better overall simulation results and increases the reliability of the model.

4.1 L-Shaped Panel Test

In this study, we utilized a coarse unstructured mesh with 1056 linear triangular elements for two simulations, one with and one without adaptive mesh reorientation. Both simulations involved the adaptive insertion of interface elements, depicted in white in Figure 3.

Figure 3-a illustrates the deformed shape from the standard analysis, which does not incorporate adaptive mesh reorientation. In this scenario, the crack, shown in red, can only propagate along the boundaries of continuum elements of the initial mesh. However, due to the mesh configuration, the crack cannot follow its true minimum energy path. Instead, it takes the lowest energy path permitted by the mesh,

which results in the crack deviating and heading towards the top left corner, as seen in Figure 3-a. In contrast, Figure 3-b presents the deformed shape of the model when adaptive mesh reorientation is employed. During this analysis, several elements near the cracked region are reoriented, highlighted in green. This reorientation allows the crack to more closely follow the true minimum energy path, resulting in a final crack path that closely approximates the ideal solution. Figure 3-c compares the load-displacement curves for both simulations. The model with adaptive mesh reorientation exhibits a lower peak load, indicating a more accurate response, while the model without reorientation shows a stiffer response with a higher peak load. This increased strength arises from the constraints imposed by the original mesh configuration, which restricts crack formation.

4.2 Single-edge Notched Tension Test

We have used a coarse unstructured mesh of 876 linear triangular elements for the 2D analysis and 15647 linear tetrahedral elements for the 3D analysis. All simulations utilized the adaptive insertion of interface elements.

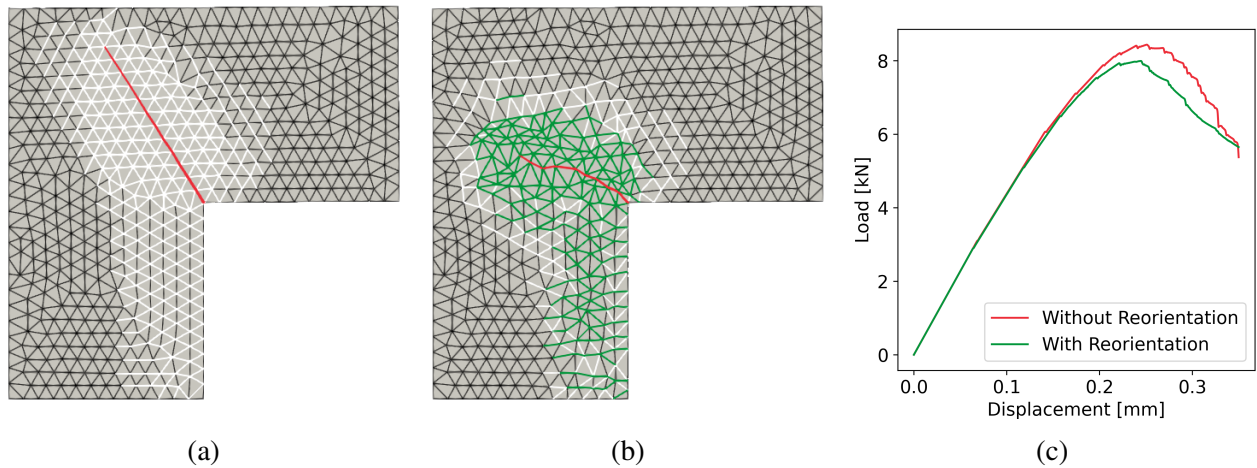


Figure 3: L-shaped panel test simulation results: (a) Standard analysis and (b) using adaptive mesh reorientation. White, green and red lines represent the unaltered, realigned and opened interface elements, respectively. (c) Load-displacement curves for both simulations. Mesh reorientation results in a more accurate crack that closely follows the experimental crack path and requires less energy, as indicated by the lower peak load in the load-displacement curve.

4.2.1 Two-dimensional analysis

Figure 4-a shows the deformed shape resulting from the standard analysis, without adaptive mesh reorientation. In contrast, Figure 4-b displays the deformed shape of the model when adaptive mesh reorientation is applied.

Similarly to the observation in Section 4.1, the standard analysis leads to a mesh-biased crack path, which deviates from the expected horizontal direction and tends downward in this case. On the other hand, the crack obtained through adaptive mesh reorientation is nearly perfectly horizontal, matching the expected crack path.

Figure 4-c compares the load-displacement curves for both simulations. The model with adaptive mesh reorientation exhibits a lower peak load, while the model without reorientation shows a higher peak load. As discussed in Section 4.1, the increased strength in the latter case arises from the constraints of the original mesh configuration, which restrict the crack's ability to follow the true minimum energy path. The lower peak load in the reoriented mesh indicates that it more effectively facilitates crack formation, requiring less energy for the crack to initiate and propagate.

4.2.2 Three-dimensional analysis

Figure 5-a shows the deformed shape from the standard analysis without adaptive mesh reorientation, while Figure 5-b depicts the deformed shape when adaptive mesh reorientation is applied.

Unlike the 2D simulation, discussed in Section 4.2.1, the adaptive mesh reorientation in this 3D case does not result in an almost horizontal crack surface as expected. However, the crack surface achieved with mesh reorientation is noticeably smoother compared to the one obtained without it. The limitation here lies in the configuration of the original mesh. While the reorientation process could realign elements by adjusting some nodes, it is constrained by the requirement to maintain a prescribed minimum mesh quality.

Despite the crack surface not being perfect, it is a clear improvement over the case without reorientation. This improvement is further evidenced in the load-displacement curves shown in Figure 5-c. The model with mesh reorientation exhibits a lower peak load, indicating that the mesh facilitated the crack formation as compared to the case without reorientation.

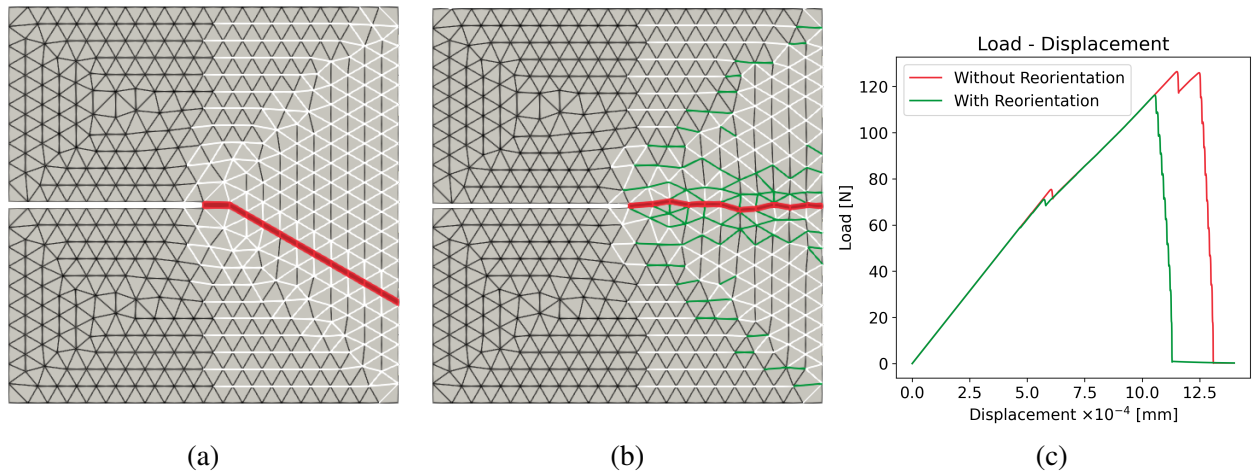


Figure 4: Single-edge notched tension test simulation results in 2D: (a) Standard analysis and (b) using adaptive mesh reorientation. White, green and red lines represent the unaltered, realigned and opened interface elements, respectively. (c) Load-displacement curves for both simulations. Mesh reorientation results in a more accurate crack that almost perfectly matches the expected horizontal crack path and requires less energy, as indicated by the lower peak load in the load-displacement curve.

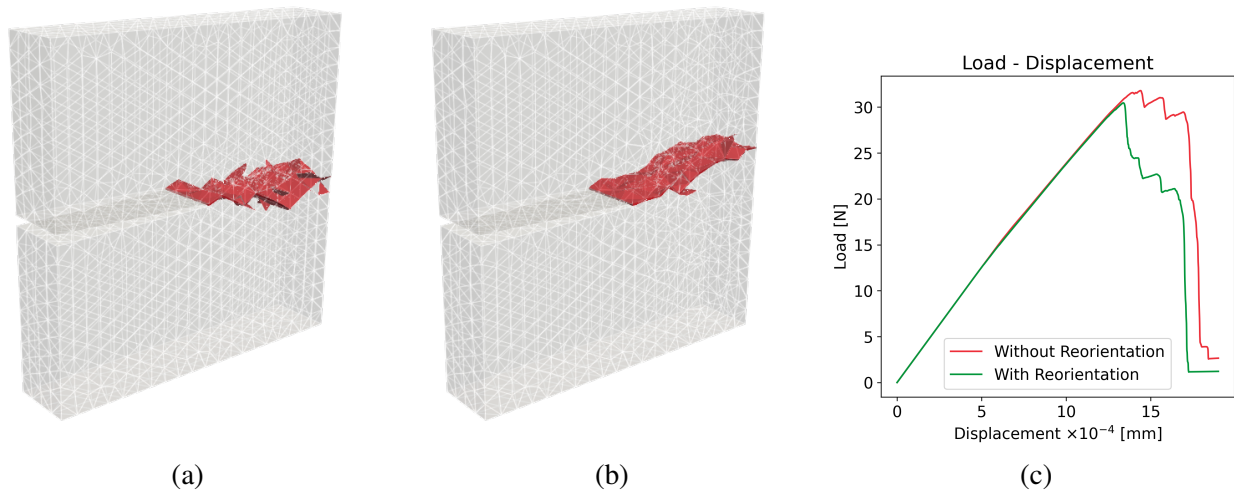


Figure 5: Single-edge notched tension test simulation results in 3D: (a) Standard analysis and (b) using adaptive mesh reorientation. Opened interface elements are shown in red. (c) Load-displacement curves for both simulations. Mesh reorientation results in a smoother crack surface that partially matches the expected horizontal crack path and requires less energy, as indicated by the lower peak load in the load-displacement curve.

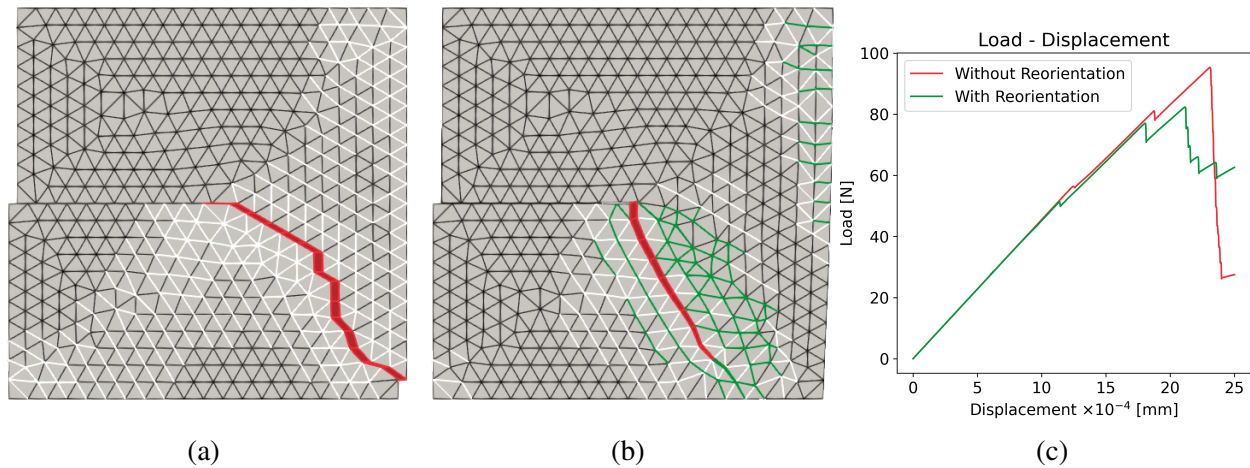


Figure 6: Single-edge notched shear test simulation results in 2D: (a) Standard analysis and (b) using adaptive mesh reorientation. White, green and red lines represent the unaltered, realigned and opened interface elements, respectively. (c) Load-displacement curves for both simulations. Mesh reorientation results in a more accurate crack that closely follows the expected crack path and requires less energy, as indicated by the lower peak load in the load-displacement curve.

4.3 Single-edge Notched Shear Test

We have used a coarse unstructured mesh of 876 linear triangular elements for the 2D analysis and 15647 linear tetrahedral elements for the 3D analysis. All simulations utilized the adaptive insertion of interface elements.

4.3.1 Two-dimensional analysis

Figure 6-a shows the deformed shape resulting from the standard analysis, without adaptive mesh reorientation. In contrast, Figure 6-b displays the deformed shape of the model when adaptive mesh reorientation is applied.

As discussed in Section 4.1, the standard analysis leads to a mesh-biased crack path, which deviates from the expected direction and tends to the bottom right corner. On the other hand, the crack path obtained through adaptive mesh reorientation is nearly in perfect agreement with the expected solution.

Figure 6-c compares the load-displacement curves for both simulations. The model with adaptive mesh reorientation exhibits a lower peak load, while the model without reorientation shows a higher peak load. As discussed in Section 4.1, the increased strength in the latter

case arises from the constraints of the original mesh configuration, which restrict the crack's ability to follow the true minimum energy path. The lower peak load in the reoriented mesh indicates that it more effectively facilitates crack formation, requiring less energy for the crack to propagate.

4.3.2 Three-dimensional analysis

Figure 7-a shows the deformed shape from the standard analysis without adaptive mesh reorientation, while Figure 7-b depicts the deformed shape when adaptive mesh reorientation is applied.

Although both crack surfaces are close to the expected crack path, the surface obtained with adaptive mesh reorientation (Figure 7-b) is significantly smoother, facilitating easier crack propagation. This is reflected in the load-displacement curve in Figure 7-c, where the simulation with reorientation exhibits a slightly lower peak load compared to the standard analysis.

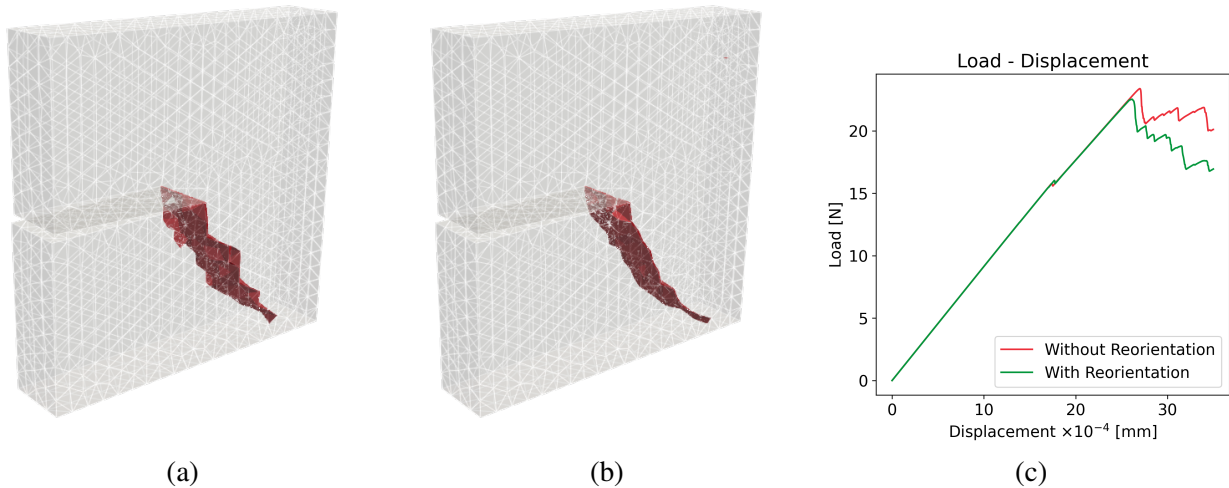


Figure 7: Single-edge notched shear test simulation results in 3D: (a) Standard analysis and (b) using adaptive mesh reorientation. Opened interface elements are shown in red. (c) Load-displacement curves for both simulations. Mesh reorientation results in a more accurate and a smoother crack surface that closely follows the expected crack path and requires less energy, as indicated by the lower peak load in the load-displacement curve.

4.4 Splitting Test

In this study, we utilized a coarse unstructured mesh consisting of 354 linear triangular elements for two simulations: one with adaptive mesh reorientation and one without. In both cases, interface elements were pre-inserted throughout the entire domain. Pre-inserting interface elements helps to mitigate potential side effects associated with the adaptive insertion, such as delayed insertion of some elements. This approach allows us to focus specifically on the impact of mesh reorientation and how it improves the results relative to the original mesh configuration.

Figure 8-a illustrates the deformed shape from the standard analysis, which does not include adaptive mesh reorientation. In this scenario, the crack, shown in red, is constrained to propagate along the boundaries of the continuum elements of the initial mesh. Due to this mesh configuration, the crack cannot follow its true minimum energy path, leading to the formation of two independent diagonal cracks.

In contrast, Figure 8-b shows the deformed shape of the model when adaptive mesh reori-

entation is applied. During this analysis, several elements near the cracked region are re-oriented, highlighted in green. This reorientation allows the crack to more closely align with the true minimum energy path, resulting in a final crack path that closely approximates the expected failure mode.

Figure 8-c compares the load-displacement curves for both simulations. The model with adaptive mesh reorientation exhibits a sudden failure, caused by the formation of a splitting crack. In contrast, the model without reorientation shows some softening due to the formation of diagonal cracks but does not experience failure, instead displaying a spurious increase in strength. This apparent high strength is a consequence of the original mesh configuration, which restricts proper crack formation.

5 CONCLUSIONS

This paper introduces the adaptive mesh reorientation algorithm, designed to enhance the crack path prediction capability of the cohesive zone cracking model using zero-thickness interface elements. While it builds on the established method of adaptive insertion of interface

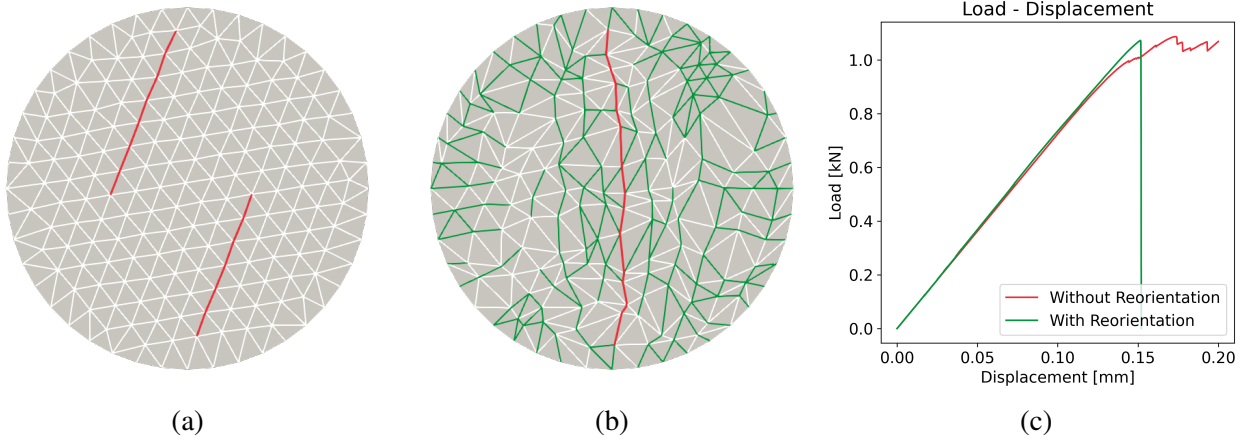


Figure 8: Splitting test simulation results: (a) Standard analysis and (b) using adaptive mesh reorientation. White, green and red lines represent the unaltered, realigned and opened interface elements, respectively. (c) Load-displacement curves for both simulations. The original mesh does not allow the formation of a single splitting crack across the specimen. Mesh reorientation allows for it, leading to sudden failure of the specimen as shown in the load-displacement curve.

elements, which is known for reducing computational costs, this proposed approach significantly improves the accuracy of crack predictions by reducing mesh-bias in crack paths, thereby enhancing the overall reliability of results obtained with the cohesive zone method.

The adaptive mesh reorientation procedure works by realigning intact interface elements to maximize their local tensile traction. This allows the elements to develop cracks with less energy. While this method primarily facilitates mode-I cracking, it also benefits scenarios involving mode-II loading, as the solid body tends to crack in mode-I (as demonstrated in Section 4.3). Nevertheless, the method does not prevent mode-II or mixed mode cracking; it simply enables elements that are about to crack in mode-I to do so in a more energetically favorable orientation. The main objective of this approach is to reduce mesh-bias in mode-I dominated crack paths, enabling cracks to overcome the limitations imposed by the initial mesh. The goal is not to achieve cracks that perfectly match analytical solutions or experimental results, but rather to improve the reliability of the well-established cohesive zone method.

Extensive testing demonstrates the effectiveness of this approach, showing consistent im-

provements in various benchmarks when comparing results with and without adaptive mesh reorientation. The reorientation consistently produces better outcomes, with improvements ranging from subtle to significant, even enabling failure modes that would otherwise be unattainable (see Section 4.4). Additionally, the proposed method is robust across both 2D and 3D applications without requiring different algorithms for each. Although not explicitly demonstrated in the tests, this method is capable of handling multiple cracks, including branching and coalescence, without the need for crack tracking. This capability arises because the method realigns intact interface elements with high traction, regardless of their position relative to existing cracks, with only one condition, which is not to affect the orientation of opened (damaged) elements. Finally, the interfaces with high-enough traction, reaching the cracking criteria, open naturally, without any intervention from the reorientation algorithm. It is worth noting that not every opened interface element is reoriented, and not every reoriented element will open. Moreover, since only intact interface elements and linear elastic bulk elements are allowed to be reoriented, the reorientation does not alter the loading history of

the structure. To our knowledge, this is the only mesh-reorientation-based discrete cracking method to predict crack paths originating from within the domain, rather than just from a singularity or the boundary.

6 ACKNOWLEDGMENTS

This research showcases computational models developed within the German Research Foundation (DFG) Priority Program 2020, Cyclic Deterioration of High-Performance Concrete in an Experimental-Virtual Lab (Project 353819637), the German Research Foundation (DFG) research grant project "3D-Druck mit Beton – numerische und experimentelle Beschreibung der Teilprozesse Extrusion, Ablage und schichtenweiser Aufbau" (Project 545131259) and the DFG-NSFC collaborative research grant program "Multiscale Tests, Simulation, Optimization and 3D Printing of UHPFRC Materials and Structures" (Project M-0172). The financial support from the DFG and the National Science Foundation of China (NSFC) is gratefully acknowledged.

REFERENCES

- [1] L. Snozzi and J. Molinari. A cohesive element model for mixed mode loading with frictional contact capability. *International Journal for Numerical Methods in Engineering*, 93(5):510–526, 2013.
- [2] V. Gudžulić, K. Daadouch, and G. Meschke. Modelling of damage processes in concrete under monotonic and cyclic loading. In *Proceedings of the 11th International Conference on Fracture Mechanics of Concrete and Concrete Structures*. IA-FraMCoS, 10-14 September 2023.
- [3] N. Schäfer, V. Gudžulić, R. Breitenbücher, and G. Meschke. Experimental and numerical investigations on high performance sfrc: Cyclic tensile loading and fatigue. *Materials (Basel, Switzerland)*, 14(24), 2021.
- [4] G. H. Paulino, W. Celes, R. Espinha, and Z. Zhang. A general topology-based framework for adaptive insertion of cohesive elements in finite element meshes. *Engineering with Computers*, 24(1):59–78, 2008.
- [5] L. Crusat, I. Carol, and D. Garolera. Application of configurational mechanics to crack propagation in quasi-brittle materials. *Engineering Fracture Mechanics*, 241:107349, 2021.
- [6] W. Celes, G. H. Paulino, and R. Espinha. A compact adjacency-based topological data structure for finite element mesh representation. *International Journal for Numerical Methods in Engineering*, 64(11):1529–1556, 2005.
- [7] K. Daadouch. Adaptive insertion of cohesive interface elements: Application to efficient macro- and mesoscale simulations of concrete cracking. Master's thesis, Ruhr University Bochum, 2021.
- [8] G. Meschke and P. Dumstorff. Energy-based modeling of cohesive and cohesionless cracks via x-fem. *Computer Methods in Applied Mechanics and Engineering*, 196(21-24):2338–2357, 2007.
- [9] M. Ambati, T. Gerasimov, and L. de Lorenzis. A review on phase-field models of brittle fracture and a new fast hybrid formulation. *Computational Mechanics*, 55(2):383–405, 2015.